Transient-State Kinetic Approach to Mechanisms of Enzymatic Catalysis

HARVEY F. FISHER*

Laboratory of Molecular Biochemistry, Veterans Affairs Medical Center, Department of Biochemistry, University of Kansas Medical Center, 4801 Linwood Boulevard, Kansas City, Missouri 64128-2226

Received July 13, 2004

ABSTRACT

Transient-state kinetics by its inherent nature can potentially provide more directly observed detailed resolution of discrete events in the mechanistic time courses of enzyme-catalyzed reactions than its more widely used steady-state counterpart. The use of the transient-state approach, however, has been severely limited by the lack of any theoretically sound and applicable basis of interpreting the virtual cornucopia of time and signal-dependent phenomena that it provides. This Account describes the basic kinetic behavior of the transient state, critically examines some currently used analytic methods, discusses the application of a new and more soundly based "resolved component transient-state time-course method" to the L-glutamate−dehydrogenase reaction, and establishes new approaches for the analysis of both single- and multiple-step substituted transient-state kinetic isotope effects.

Introduction

It may be said that nature has provided scientists with enzymes as a way of teaching us the basic principles of physical organic chemistry. If so, our current understanding of the catalytic power of enzymes suggests that we have thus far completed much less than one-thousandth of the course. Aside from providing advanced lessons in the nature of catalysis (which is itself a major topic of interest to chemists), properly resolved enzyme mechanisms may offer fresh insights into the nature of transition states as well as that of covalent bond formation and breaking events. In 1949, at a time well before X-ray crystallography had revealed the structure of enzymes and the basis of their enormous catalytic power was widely ascribed to some unknown source present only in biological systems, Frank Westheimer opined that enzyme action was based on the same basic principles inherent in classical organic chemical reactions but that enzymes were far more gifted in applying them than were the best scientists of our time. He went on to predict that an enzyme must be an entity that can apply concentrated HCl to one side of a substrate atom while simultaneously adding concentrated NaOH to the opposite side of the same atom without producing NaCl.[1] Time has rendered Westheimer's heretical statements into truisms exemplified in a later section of this Account.

The general approach to the problem of mechanisms of enzymatic catalysis has been to combine the results of kinetic measurements with those of X-ray crystallography and NMR-based structures and relating the two using chemical intuition. While such structural studies have already provided a wealth of information of increasing resolution, they are necessarily largely limited to static complexes requiring rather long intuitive leaps to deduce the structures of the reactive complexes, which comprise the heart of the catalytic mechanism.

Thus far, most of our kinetic knowledge of enzymic catalysis has been based on steady-state measurements. The power of this approach lies in the elegant rigorous algebraic theory, which underlies its application. Its initial limitation, a lack of sensitivity to central complex interconversion steps, has been progressively reduced by the use of inhibitors, the pH dependence of its parameters, and most strikingly the ingenious application of a wide

Harvey F. Fisher was born in Cleveland, Ohio in 1923. He obtained a B.S. in Chemistry from Western Reserve University in 1947 and a Ph.D. in Biochemistry from the University of Chicago in 1952 under the direction of Professors Birgit Vennesland and Frank H. Westheimer. After postdoctoral work under David Rittenberg at Columbia University and Robert Alberty at the University of Wisconsin, he served as an Instructor in chemistry at the University of Massachusetts and as a Senior Scientist at the Edsel B. Ford Institute in Detroit. In 1963, he joined the Department of Biochemistry of the University of Kansas School of Medicine, where he is currently a Professor and Director of the Laboratory of Molecular Biochemistry at the Kansas City Veterans Administration. His research involves the application of physical, chemical, and biophysical approaches to the study of mechanisms of enzymatic catalysis.

variety of kinetic isotope effects.[2,3] While much has been learned in this way, such results are by their nature indirect. The transient-state kinetic approach, on the other hand, permits the direct observation of the time courses of individual reactive intermediates in real time. Such a study, in principle, provides as its immediate output the mechanistic picture that is the ultimate goal of the steady-state approach. The difference is due to the fact that steady-state parameters are by definition independent of both signal and time, while transient-state signals are strongly dependent on both signal and time, providing a wealth of specific phenomena limited only by the ingenuity of the experimentalist. Given the increasing availability of the required instrumentation in chemistry and biochemistry departments, why then has such a powerful approach not been more widely used? The answer to this question lies largely in the lack of the body of applicable and rigorously derived theory of the sort that underlies steady-state kinetics. Here, we describe some initial attempts to establish the basis of such a theory.

Transient-State Experimental Approaches

While a number of different approaches to the direct detection of the pre-steady-state events in enzymatic reactions have been employed over the years, two methods predominate currently. (1) In the stopped-flow method, the reaction is initiated by forcing two reactant solutions through a mixing device past an optical detector with an abrupt stoppage of the flow. Changes in the signal after a 1−2 ms dead time are then followed as a function in time. The method has been described in detail by Hiromi.[4] (2) In the quench-flow technique, a similar method is used to generate a flowing reaction mixture that is stopped abruptly at various points in time after initiation by rapid introduction of any of a variety of reaction-quenching solutions that serve to both stop the reaction and precipitate the protein. The supernatant solution is then analyzed for the concentrations of various products present at the quenching time. This approach is discussed in a volume by Johnson.[5] Each of these methods has its strengths and limitations. Each presents pictures of the same chemical events in time from different viewpoints. The stopped-flow technique has the potential of detecting both known and unexpected intermediates quite generally throughout the catalytic time course but bears the burden of distinguishing between contributions from several components to an observed signal. The quench-flow technique, conversely, provides much greater certainty as to the identity of an observed species (as discussed by Palfey in ref 5) but is generally limited in its application to product-release steps. Thus, they are best viewed as complementary techniques.

Behavior of Transient-State Reactions

Transient-state reactions are typically run under conditions where all reactants are initially at saturating concentrations to eliminate any complexities arising from ligand-binding steps and to provide maximal concentra-
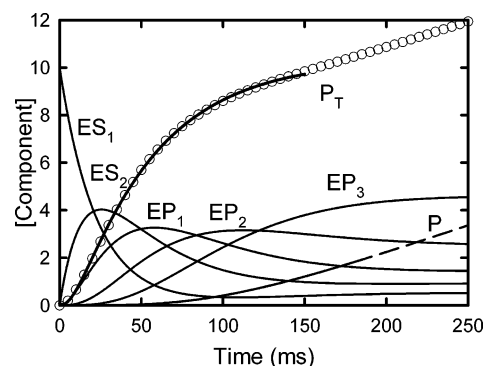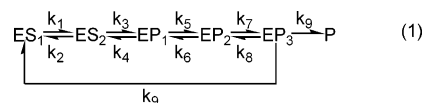
FIGURE 1. Time courses of individual enzyme complexes for the reaction shown in eq 1, where $k_1 = 45$, $k_2 = 1$, $k_3 = 40$, $k_4 = 10$, $k_5 = 30$, $k_6 = 8$, $k_7 = 20$, $k_8 = 6$, and $k_9 = 5$. The dashed segment of curve P indicates the onset of classical steady-state product release. The P_T curve (○) represents the sum of all product forms. The solid line represents a two-exponential fit to these data of eq 8, where $\lambda_1 = 116$ s^{-1} and $\lambda_2 = 20$ s^{-1}.

tions of central complexes. (The "single turnover" approach, in which the concentration of one reactant is held to less than that of the enzyme itself, necessarily includes such steps, adding some detail to a phase emphasized in steady-state studies. As such, it lies outside of the scope of this Account.) A reaction run under such saturating conditions may be expressed simply as where S and P

$$ES_1 \underset{k_2}{\overset{k_1}{\rightleftharpoons}} ES_2 \underset{k_4}{\overset{k_3}{\rightleftharpoons}} EP_1 \underset{k_6}{\overset{k_5}{\rightleftharpoons}} EP_2 \underset{k_8}{\overset{k_7}{\rightleftharpoons}} EP_3 \overset{k_9}{\rightarrow} P \qquad (1)$$

$$k_9$$

represent the substrate and product, respectively. Ligand molecules entering or leaving a complex at a given point along the reaction time course can be easily accommodated by minor modifications of the scheme. From the mass law, the time-dependent behavior of each component of the reaction such as EP_1 for example, may be written as

$$d[EP_1]/dt = k_3[ES_2] + k_6[EP_2] - (k_4 + k_5)[EP_1] \quad (2)$$

It is at this point that the steady-state and transient-state approaches diverge. The basis of the steady-state approach is the assumption that at the time of measurement $d[X]/dt$ is zero for *all* complexes, an assumption that is justified within a few seconds after mixing. With this assumption, the entire set of equations of the form of eq 2 assume a relatively simple algebraic form. In the transient state, however, this condition is not met generally throughout the time of measurement and each $d[X]/dt$ value is a time-dependent function.

While an explicit integrated equation representing a reaction of the complexity of that shown in eq 1 has been formally proven to be mathematically impossible, numerical integration of the set of n differential equations for a reaction of n intermediates is easily obtained using any a number of available computer programs (such as SCIENTIST). The results of such a calculation for the reaction of eq 1 are shown in Figure 1. It can be seen that the time

course of each product complex involves the following series of phases: (a) a lag phase during which only a small amount of the component is produced, (b) an acceleration phase (frequently referred to as the "burst"), (c) an initial local steady-state phase (which may be lengthy or only momentary), (d) a deceleration phase, leading to (e) a second local steady state, and finally, when all components have reached their final steady state, (f) the time-linear release of the product as defined in formal steady-state terms. It is important to note the distinction between the several local component steady states and the global condition required by the steady-state kinetic theorems.

The shape of the signal observed experimentally from the typical enzyme reaction portrayed in eq 1 will depend on the relative extinction coefficients (or other corresponding intensive properties) of the various complexes involved in the reaction. Thus, at any point in time, the total product concentration is $[P_t] = a[ES_1] + b[ES_2] + c[EP_1] + d[EP_2] + e[P]$, where the extinction coefficients, $a = 0$, $b = 0$, and c, d, and e are all equal. The observed signal is indicated by the series of open circles. The dashed portion of the curve designated as P represents the onset of the classical steady state.

Kinetic Analysis of Reactions in the Transient State

As we have noted, the formal mathematical integration of the set of equations of the form of eq 2, which is required to represent the time courses of each individual component of the reaction shown in eq 1, is limited to the reversible two-step equation

$$A \underset{k_2}{\overset{k_1}{\rightleftharpoons}} B \underset{k_4}{\overset{k_3}{\rightleftharpoons}} C \tag{3}$$

While such a reaction is mechanistically insufficient for any realistic enzyme reaction, examination of its mathematical solution illuminates several fundamental properties that are applicable to the general case shown in eq 1. The general solution for the time dependencies of components B and C in eq 3 is[6]

$$[B](t) = k_1\left(\frac{k_4}{\lambda_1\lambda_2} + \frac{k_4 - \lambda_1}{\lambda_2(\lambda_1 - \lambda_2)}\right)e^{-\lambda_1 t} + k_1\frac{\lambda_2 - k_4}{\lambda_2(\lambda_1 - \lambda_2)}e^{-\lambda_2 t} \tag{4}$$

$$[C](t) = k_1 k_3\left[\frac{1}{\lambda_1\lambda_2} + \frac{e^{-\lambda_1 t}}{\lambda_1(\lambda_1 - \lambda_2)} - \frac{e^{-\lambda_2 t}}{\lambda_2(\lambda_1 - \lambda_2)}\right] \tag{5}$$

where

$$\lambda_1 = \frac{1}{2}(p + q) \quad \lambda_2 = \frac{1}{2}(p - q) \tag{6}$$

and

$$p = k_1 + k_2 + k_3 + k_4$$
$$q = \sqrt{p^2 - 4(k_1 k_3 + k_2 k_4 + k_1 k_4)} \tag{7}$$

It is important to note that λ_1 and λ_2 of eq 6 are, in fact, the values of the two exponential terms $e^{-\lambda_1 t}$ and $e^{-\lambda_2 t}$ that would be obtained by the customary fitting of experimental results to the phenomenological equation

$$f = a_0 + a_1 e^{-\lambda_1 t} + a_2 e^{-\lambda_2 t} \tag{8}$$

Regrettably, it has become a wide-spread occurrence in the current literature that highly respected authors writing in first-line scientific journals make the fallacious assumption that such λ values may be equated with specific rate constants. Such assumptions are totally baseless for two quite independent reasons: (1) it can be seen from eqs 6 and 7 that even in the simple two-step reaction shown in eq 3 that the two experimentally observable exponential λ actually correspond to the complex equations

$$\lambda_1 = \frac{k_1 + k_2 + k_3 + k_4 + \sqrt{(k_1 + k_2 + k_3 + k_4)^2 - 4(k_1 k_3 + k_2 k_4 + k_1 k_4)}}{2} \tag{9}$$

$$\lambda_2 = \frac{k_1 + k_2 + k_3 + k_4 - \sqrt{(k_1 + k_2 + k_3 + k_4)^2 - 4(k_1 k_3 + k_2 k_4 + k_1 k_4)}}{2} \tag{10}$$
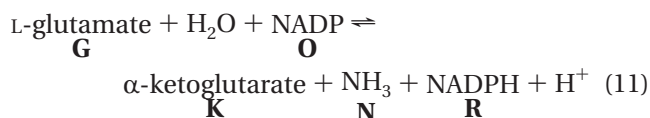
It is apparent from eqs 9 and 10 that the expression for each one of the two λ values contains contributions from every single rate constant in the equation for the overall reaction and that each constant occurs in multiple terms of substantial complexity. Clearly, λ_1 has no obvious relationship to k_1. When quite reasonable sets of rate constants are applied to eqs 9 and 10, it can be shown that k_1 and λ_1 (or k_2 and λ_2) may differ by an order of magnitude. Indeed, $\lambda_1 = k_1$ only if $k_2 = 0$ (in which case, $\lambda_2 = k_3 + k_4$). This very point was made by Schoepfer et al. in 1988,[7] but it appears to have been generally disregarded. (2) Bernasconi[8] has pointed out the difficulty in distinguishing exponential terms differing by any factor less than 6 in a reaction time course. It was indeed this very difficulty that severely impaired the applicability of the once promising temperature-jump (or relaxation) approach to reaction kinetics. As shown in Figure 1, the burst phase of the total product signal of a five-step reaction can be fitted with high precision by the simple two-exponential form of eq 8. In this case, λ_1 is 2.25 times the value of the actual k_1, further confounding any physical interpretation of such phenomenological values.

Having described the phenomenological transient-state behavior of the general multistep reaction shown in eq 1 and having examined the mathematical basis of that behavior, we now proceed to develop a general approach to the problem of translating transient-state experimental data into mechanistic terms. The kinetic solution to eq 1 requires the simultaneous integration of the complete set of n independent differential equations of the form of eq 2 for a reaction of n steps, where the $d[X]/dt$ terms have finite values. To solve this complex problem of translating

transient-state experimental data into mechanistically interpretable kinetic equations, we have developed an approach, as discussed in refs 9–11, which we believe to be quite rigorous and free of the limitations of current practices in transient-state methods. This method, "the resolved component time-course approach", employs the following basic experiment: a transient-state absorbance versus a wavelength and time array is obtained using a stopped-flow apparatus to assemble a series of side-by-side single wavelength time traces in which a solution containing enzyme and one substrate in one syringe is mixed with a solution containing a second substrate and an equal concentration of enzyme in the other. The apparatus is operated under computer control and measures a series of time courses at decreasing fixed wavelengths. The analysis of the resulting array requires three successive operations: (1) The deconvolution process involves the selection of sequential fixed-time slices of the array, each of which represents the absorbance spectrum of the solution at some time "*t*" and the reiterative solution of a multiwavelength determinant of Beer's law equations. We supply the spectra of known enzyme complexes as putative inputs in this process and shift those models under rigorous rules until their sum approaches a solution whose residuals are wavelength-independent. This process provides a set of the time courses of individual components. (2) Next, the individual components are tentatively assigned to appropriate locations in eq 1. (3) The resulting set of numerically integrated forms of eq 1 are then set in a matrix form and iteratively solved to obtain a simultaneous fit to the set of experimentally determined component time courses. A satisfactory fit establishes the kinetic competence of the proposed reaction mechanism. The failure to obtain such a satisfactory fit requires modification of the reaction scheme. The set of rate constants provided even by a satisfactory fit are not necessarily unique, and no significance should be attributed to the values of the individual microconstants so obtained. Therefore, to apply a further constraint to the solution, one may solve the data from an α-deutero substrate and from an α-protio one simultaneously, permitting only the two constants of the hydride transfer step to vary. Solving the now highly constrained set of differential equations by means of computer-run matrix manipulation provides a very exacting test of a proposed mechanism. Time courses measuring fluorescence excited at various wavelengths may differ phenomenologically from their absorbance counterparts, either further constraining the overall kinetic fit or, alternatively, providing evidence of previously unsuspected complexes.[12] The time courses of signals unique to a specific species (such as the release of protons measured by an indicator dye[13]) and those provided by a quench-flow experiment under identical reaction conditions may provide further mechanistic detail. The effect of varying pH on transient-state reactions reveals p*K* shifts of specific reactive intermediates, resolving ambiguities inherent in steady-state studies.[14]

Application of the Approach to the Glutamate Dehydrogenase (GDH) Catalyzed Reaction

The pyridine nucleotide-linked oxidative deamination of L-glutamate catalyzed by GDH has the following stoichiometry:

$$\text{L-glutamate} + H_2O + NADP \rightleftharpoons$$
$$\mathbf{G} \qquad\qquad \mathbf{O}$$
$$\alpha\text{-ketoglutarate} + NH_3 + NADPH + H^+ \quad (11)$$
$$\mathbf{K} \qquad\qquad \mathbf{N} \qquad\quad \mathbf{R}$$

The bold letters shown below each species will be used throughout this Account, where **G** is L-glutamate, **K** is α-ketoglutarate, **N** is ammonia, **O** is NADP (oxidized coenzyme), and **R** is NADPH (reduced coenzyme). The basic chemical mechanism is now generally assumed to be

$$(12)$$
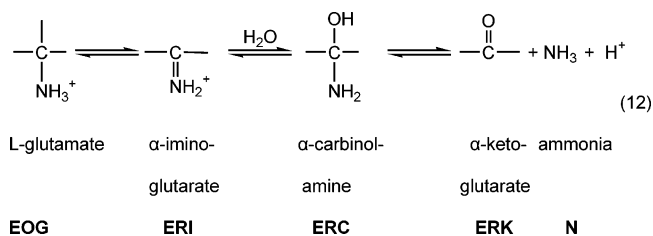
where **I** is α-iminoglutarate, **C** is α-carbinolamine, and **E** is the enzyme. The existence of the α-imino acid complex as an intermediate in the reaction was established by our work using O[18] exchange[15] and by our demonstration of the catalysis by bovine liver L-glutamate dehydrogenase (blGDH) of the NADPH reduction of a cyclic imino acid (Δ^1pyrrolidone carboxylic acid) to L-proline, a reaction, which, in the absence of enzyme, proceeds spontaneously at a slow rate.[16] In a subsequent study of both primary and secondary deuterium isotope effects, in both the spontaneous and the blGDH-catalyzed reactions,[17] we concluded that the hydride transfer occurs in a single rate-limiting step, that the transition state in the enzymatic reaction is more symmetrical in the enzyme-catalyzed reaction than the product-like state in the spontaneous reaction, that both of the C4 hydrogens of NADPH participate in the reaction coordinate motion, and that there was evidence of some degree of tunneling. Rife and Cleland's steady-state kinetic studies led them to propose the sequence shown in eq 12.[18] They also postulated that a proton of the substrate must be transferred to an acidic group on the enzyme prior to the hydride transfer step and that a water molecule must be bound to a basic group in a position close enough to permit a nucleophilic attack by its oxygen atom on the α-carbon atom of the resulting α-imino acid to form the carbinolamine. Equation 12 is, in fact, the mechanism they first proposed. This prescient prediction was proven to be correct in atomic detail to within 1 Å by the X-ray crystal structure of a corresponding bacterial form of GDH.[19]

Time courses of the reaction at selected wavelengths and the corresponding "time-slice" spectra are shown in Figure 2. The resolution of such time slices, accomplished by a Beer's law fitting of the established model spectra
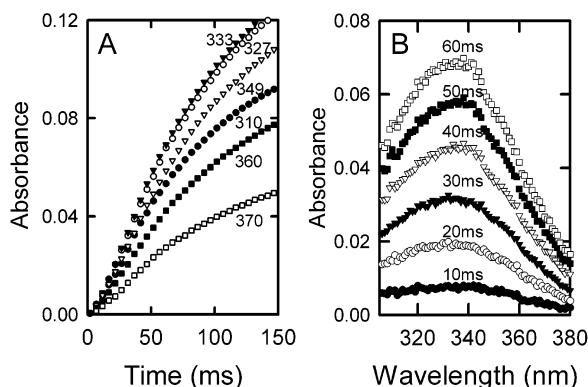
FIGURE 2. Selected slices of the absorbance versus time and wavelength array observed in a blGDH-catalyzed reaction. (A) Fixed-wavelength time courses. (B) Fixed-time spectra of the same array.
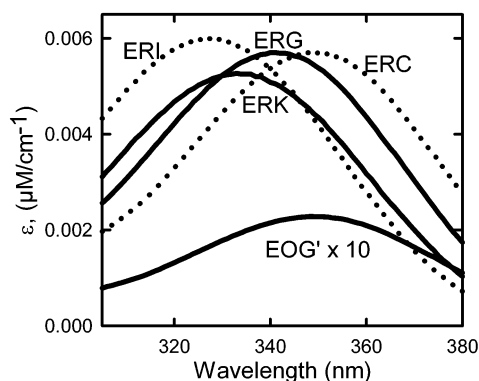

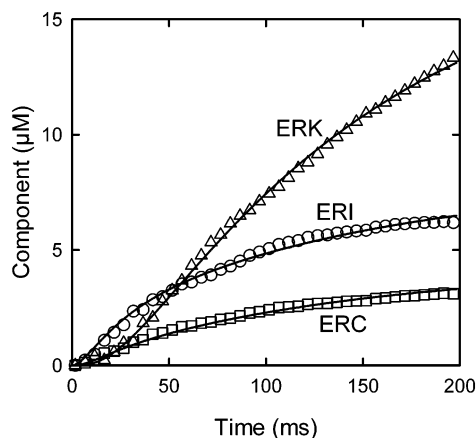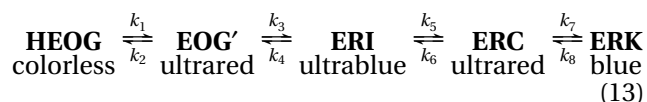**FIGURE 3.** Spectra of known (—) and inferred (···) complexes.

FIGURE 4. Resolved component time courses obtained from the data of Figure 2. The solid lines represent fits of eq 5 to the data.

shown in Figure 3, produces the set of component time courses shown in Figure 4. These fits are necessary and sufficient to establish the kinetic competence of the following minimal reaction sequence:

$$\underset{\text{colorless}}{\textbf{HEOG}} \overset{k_1}{\underset{k_2}{\rightleftharpoons}} \underset{\text{ultrared}}{\textbf{EOG}'} \overset{k_3}{\underset{k_4}{\rightleftharpoons}} \underset{\text{ultrablue}}{\textbf{ERI}} \overset{k_5}{\underset{k_6}{\rightleftharpoons}} \underset{\text{ultrared}}{\textbf{ERC}} \overset{k_7}{\underset{k_8}{\rightleftharpoons}} \underset{\text{blue}}{\textbf{ERK}}$$
(13)

On the basis of these results, supplemented by transient-state fluorescence,[12] pH,[14] and ammonia jump studies, we conclude that an initial "colorless" **HEOG** complex (in

which the catalytic lysine 126 is still protonated) is formed in the instrumental dead time. In the next step, lysine 126 of **HEOG** loses its proton to form **EOG′**, a weakly absorbing charge-transfer complex characterized by a very highly red-shifted fluorescence. After closure of the cleft, hydride transfer to NADP occurs, forming **ERI**, a highly blue-shifted α-iminoglutarate complex. A nucleophilic attack by the Iysyl-bound water molecule now occurs leading to the formation of **ERC**, a highly red-shifted α-carbinol-amine complex. NH_3 leaves at this point, an event that we have not yet measured directly, but which is supported by the results of our "ammonia jump" studies. This produces the moderately blue-shifted **ERK** α-ketoglutarate complex. It can be seen that no significant amount of free **R** is produced in the 0−200 ms time range.

Conformational Changes

There is now ample evidence for the occurrence of protein domain motions resulting in active-site opening and closing events as integral features of enzyme-catalyzed reactions. Crystal structures for three distinctly different states of active-site closure have been obtained for a bacterial GDH.[19] Isothermal calorimetric studies from this laboratory[20] and that of Biltonen[21] have established that the ubiquitous large negative heat capacities observed in protein ligand binding reactions can be explained by hidden cleft-closure events characterized by $\Delta H°$ values of ∼23 kcal M^{-1} and widely varying $\Delta G°$ values. The mechanistic role for such events may be easily visualized; the active site must be open at various times to permit the entry of reactants and the departure of products. It must be closed at other times to provide the hydrophobic environment required for chemical events such as hydride transfer and nucleophilic addition. It is also obvious that necessary hydrogen bonding between functional groups on the surfaces of active-site clefts would be disrupted by an aqueous environment. For a full understanding of an enzyme mechanism, therefore, it is essential that we find a means of determining the kinetic contributions of these events and establishing their precise locations on the reaction scheme. For this, we require a kinetic method to utilize the detailed but necessarily static evidence that we have described above. Steady-state kinetics is well able to determine the order of addition and departure of substrates and products (including H_2O and H^+), but it lacks the mechanistic precision required to pinpoint the precise steps at which these individual events occur. Transient-state kinetics, however, can provide such information; we describe two different experimental approaches to the problem.

pH Jump Approach. Commercially available stopped-flow spectrophotometers are now quite generally provided with a "multimixing" device, which permits the rapid injection of a second solution at various selected points in time into an ongoing transient-state reaction. Using this feature, we jump a weakly buffered solution reacting at one pH with a shot of a substrate-containing solution at a different pH at a series of varying delay times. We then
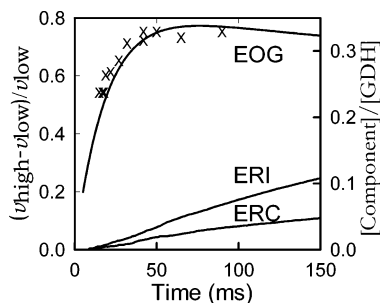
FIGURE 5. Comparison of pH jump results with blGDH component time courses. A premixed **E**, **O**, and **G** solution reacting at pH 6.2 was jumped at different delay times with the same glutamate solution at pH 8.5 (pH 6.2 for control experiments) to provide a final pH of 7.1. The pH jump data points (×) indicate the ratio of the difference of initial rates for the pH jump and control experiments to that of the control rates.
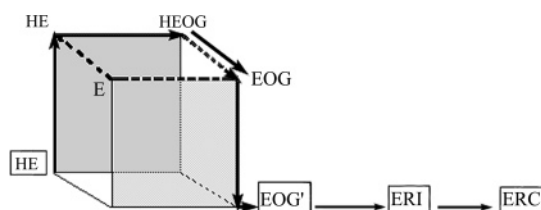

FIGURE 6. Conformational states of the blGDH reaction. The back faces of the cubes indicate the protonated species, and the front faces indicate the unprotonated species, respectively. The enclosed species indicate closed enzyme complexes, and the open species indicate those in the open phase. The thick arrow lines indicate the reaction pathway at low pH. The dashed thick lines indicate the reaction course following the pH jump.

measure the relative initial change in the rate of formation of the various individual reactive complexes that we can identify. The dilution effect of the jump is corrected for by a control experiment, where the jump solution is at the same pH as the reacting mixture. The maximal rate effect that could have been achieved is calculated from the initial rate of the unjumped reaction at the final pH of the jump reaction. The results of such an experiment are shown in Figure 5, superimposed on a plot of component time courses resolved from an identical "non-jumped" reaction.[22] The precise correspondence of the fractional jump amplitudes to the time course of the **EOG′**

complex provides evidence for the existence of a previously undetected prehydride-transfer open-form complex, whose formation must precede that of the necessarily closed charge-transfer complex (**EOG′**), which we have identified by its weakly absorbing highly fluorescent behavior.[12] We have been able to combine these findings with known kinetic features to provide a detailed picture of the prehydride phase of the reaction as shown in Figure 6. This approach is not limited to pH effects. Jumps using products will indicate any points on the reaction time courses where the active site is open and the specific binding site for that product is unoccupied.

Spectroscopic Detection of Transient-State Domain Motions. Our initial resolution of the transient-state spectra of *Clostridium symbiosum* glutamate dehydrogenase (csGDH),[11] (shown in Figure 7A) appeared to indicate the release of free NADH at a mechanistically unlikely point. Using lactic dehydrogenase (which rapidly binds NADH to form a tight blue-shifted complex) as a reporter group for free NADH, we found that the early portion of the unshifted NADH component could not represent free NADH as shown in Figure 7B. It could, however, be accounted for by some combination of open-cleft forms of **ERI**, **ERC**, and **ERK** in which the reduced nicotinamide chromophore of NADH is exposed to the aqueous solvent. Such an environment might well fail to induce the substantial red or blue shifts observed in the closed forms of the enzyme where the chromophore is enclosed in a hydrophobic environment. Ascribing this component to open forms of any of a number of enzyme−NADH−ligand forms on this basis, we obtained a satisfactory and kinetically competent fit to a reaction scheme, which includes both open and closed forms of **ERI**, **ERC**, and **ERK** complexes as shown in Figure 7C. This conformational reaction time course (which differs considerably from that of the highly homologous blGDH) was supported by pH jump studies, which showed that the csGDH active site is about 95% open throughout the reaction.[23]

Mechanistic Variations

We have observed striking variations in the transient-state kinetic behavior of three α-amino acid dehydrogenases
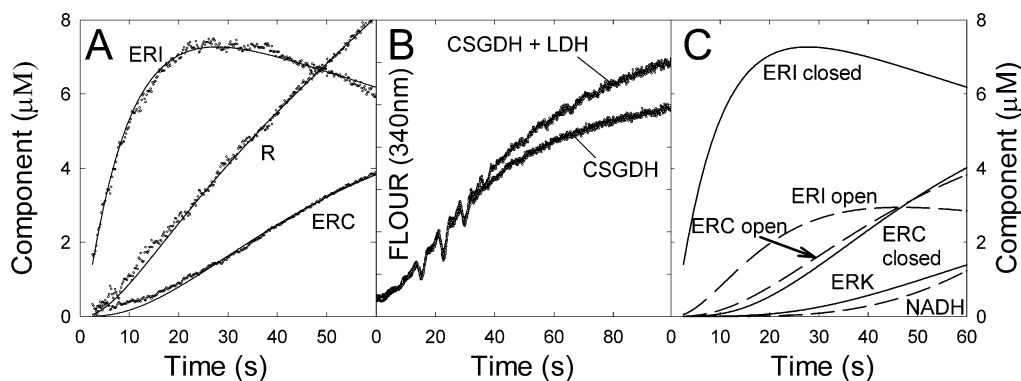

FIGURE 7. Resolution of a free "**R**" signal in a csGDH reaction. (A) Component time courses. (B) Effect of lactic dehydrogenase on the fluorescence time course. (C) Resolved component time courses. Solid lines indicate closed complexes, and dashed lines indicate open forms.
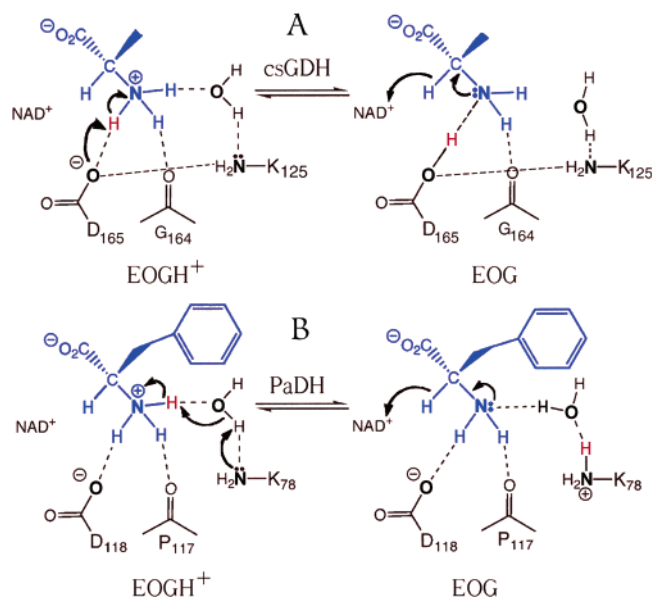
FIGURE 8. Comparison of the mechanisms of a single step in the reactions of two homologous α-amino acid dehydrogenases. (A) csGDH. (B) PaDH. Adapted from ref 24. Substrate atoms are indicated in blue, and the transferred α-amino hydrogen atom is indicated in red. The bolded letters designate the atoms of the catalytic tetrad in the text.

whose active-site functional-group geometries are identical within 1 Å, whose steady-state kinetic parameters (including pK values) differ little, and whose gross mechanisms appear to involve the same sequences of intermediate complexes of similar spectroscopic properties. Some of these phenomenological differences (such as the pre- and posthydride transfer step location of proton release in the blGDH and csGDH reactions) may be ascribed to differences in their conformational time courses as we have just discussed. The basis of other differences, however, remains obscure. Recently, we have noted the existence of a four-atom nearly square and planar tetrad of atoms consisting of a nitrogen atom of an enzyme lysine ε-amino residue, an oxygen atom from an enzyme aspartate carboxylate residue, a nitrogen atom from the substrate α-amino group, and an oxygen atom from a tightly bound water molecule.[28] The geometry of this tetrad is such that subangstrom variations in their interatom distances can produce any of 27 different hydrogen-bonding patterns in a given intermediate complex. A documented example of the ability of this tetrad to act as a mechanistic switching device is shown in Figure 8. It is well-established that a proton from the α-NH$_3^+$ group of the bound substrate must be removed prior to the hydride transfer step in the reactions of this class of enzymes. In the csGDH reaction, as shown in Figure 8A, an oxygen atom from an aspartyl carboxylate group hydrogen bonded to the lysyl nitrogen atom of the tetrad is poised in the proper position to accept this proton (as predicted earlier by Rife and Cleland[18]). However, as shown in Figure 8B, a high-resolution structure of phenylalanine dehydrogenase (PaDH) indicates the presence of the same tetrad with only subangstrom differences in geometry between it and its csGDH counterpart.[24] These minute differences,
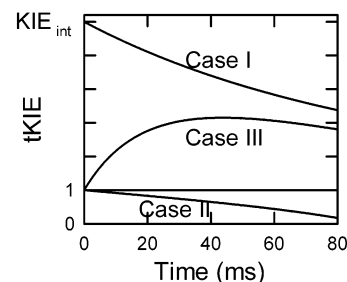

FIGURE 9. Theoretical tKIEs for a$(dv/dt)_H/(dv/dt)_D$ for the cases: I, only post (blGDH) hydride species; II, only prehydride species; or III, both species contributing to the signal.

however, are sufficient to abolish the aspartyl−lysyl hydrogen bond and to increase the distance between the α-amino nitrogen hydrogen atom and the aspartyl oxygen atom by 0.5 Å, precluding its function as a hydrogen acceptor. The substrate proton is in this case transferred to the lysyl group of the tetrad through the bridge provided by its bound water molecule, reversing the direction of the electron flow from clockwise in the csGDH reaction to counterclockwise in the PaDH reaction. It may be noted that this tetradic structure supports Westheimer's prediction providing local concentrations of H$^+$ and O$^-$ of greater than 50 M at the substrate α-C atom! A new approach to following this sort of proton motion in the transient state follows.

Kinetic Isotope Effects (KIEs) in the Transient State

Single-Step-Substituted Case. Transient-state KIEs (tKIEs) are strongly dependent on both the time and the signal measured. Since the first tKIE for an enzyme reaction reported in our 1970 paper,[25] no rigorous theory for the interpretation of tKIEs had been available. We have now derived such a soundly based theory[26] and have demonstrated its application to experimental data. Defining a transient-state KIE as

$$\text{tKIE}(t) = \frac{d[S_H]/dt}{d[S_D]/dt}$$

where S is the observed signal, we have formally proven that, for any range of numerical values for the rate constants and the intrinsic forward and reverse KIEs, the behavior of any observed transient signal must obey the following three absolute rules as shown in Figure 9: (Case I) Only the posthydride transfer species contributes to the signal. In this case, the observed tKIE curve must start at the intrinsic KIE at zero time and must then decrease continuously with time. (Case II) Only the prehydride transfer species contributes to the signal. In this case, the observed tKIE curve must start at a value of unity at zero time and then must continuously decrease with time. (Case III) Both pre- and posthydride transfer species contribute to the signal. In this case, the observed tKIE curve must start at a value of unity at zero time and then will either rise to a maximum and then fall or fall to a minimum and then rise. We have applied this approach
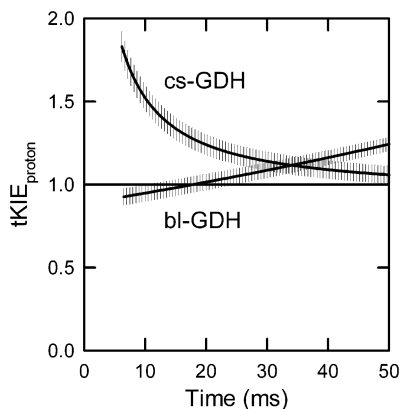
FIGURE 10. Time courses of KIE$_{obs}$ for proton release in the reactions catalyzed by csGDH and blGDH.

experimentally to demonstrate a reversal in the sequence of steps in the reactions catalyzed by two structurally homologous forms of GDH.[23] As shown in Figure 10, stopped-flow indicator dye experiments with α-H and α-D L-glutamate prove that in the blGDH reaction case II behavior is observed, indicating that proton release precedes the hydride-transfer step. (The small slow rise in time of the tKIE suggests the presence of small pK shifts between the various posthydride transfer complexes.) In the reaction of the homologous bacterial enzyme (csGDH), case I behavior is observed, showing that proton release occurs after the hydride transfer step. It is interesting to note that the steady-state patterns of the two enzymes are similar, both showing the same pK value of 8.

Multistep-Substituted Case. We have now extended this transient-state KIE theory to include the general case shown in eq 14, where each step of the reaction may be subject to an isotope effect (as in D$_2$O solvent isotope studies).[27]
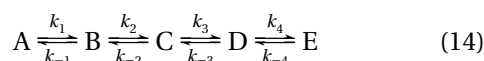
$$A \underset{k_{-1}}{\overset{k_1}{\rightleftharpoons}} B \underset{k_{-2}}{\overset{k_2}{\rightleftharpoons}} C \underset{k_{-3}}{\overset{k_3}{\rightleftharpoons}} D \underset{k_{-4}}{\overset{k_4}{\rightleftharpoons}} E \qquad (14)$$

Figure 11 shows the results of the application of numerical integration to the differential equations repre-

senting this reaction sequence for an arbitrary set of assumed parameters. Figure 11a shows the time course of each component. The solid line indicates the unsubstituted case, while the dashed lines shows the time courses of each of the corresponding components assuming the effects of various arbitrarily chosen KIEs on each forward and reverse rate constant.

Applying the definition

$$\text{tKIE}_X(t) = \frac{d[X_H]/dt}{d[X_D]/dt}$$

to the pairs of H and D component time courses of (Figure 11a) (using numerical differentiation), we display the resulting tKIE$_X(t)$ time courses for each component in Figure 11b. The intercept of each tKIE$_X(t)$ curve on the $t = 0$ axis represents the tKIE$_X^0$ value for component X as defined by

$$\text{tKIE}_X^0 = \lim_{t \to 0} \text{tKIE}_X(t)$$

[The concept that a component defined as having a concentration of 0 at $t = 0$ can have a finite value for its first derivative of its concentration at $t = 0$, which may appear to be counterintuitive. However, the limit of a function as $t \to 0$ is not necessarily its value at $t = 0$. Further, tKIE$_X^0$ measures the *ratio* of the derivatives of the H and D time courses as t approaches 0. In general, this ratio is a finite number]. Examination of the 0 time intercepts of the various component time courses shows that in general tKIE$_X^0$ does not equal the intrinsic (KIE$_{X,int}$) value assumed for that step but rather leads us to propose three theorems.

The first theorem may be stated formally as

$$\text{tKIE}_i^0 = \prod_{i=1}^{n} \text{KIE}_{i,int} \qquad (15)$$

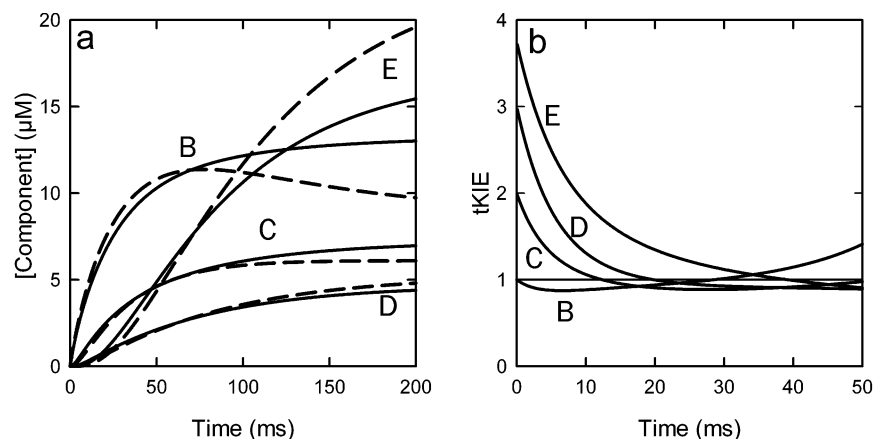**FIGURE 11.** Time dependence of tKIE$_X(t)$ in the general sequential reaction shown in eq 5. (a) Solid and dashed lines indicate the time courses for [B], [C], [D], and [E] for the nonisotopically substituted and multistep isotopically substituted reaction, respectively, assuming the following KIE$_{int}$ values: KIE$_{1,int}$ = 1, KIE$_{2,int}$ = 2, KIE$_{3,int}$ = 1.5, KIE$_{4,int}$ = 1.25, KIE$_{-1,int}$ = 1, KIE$_{-2,int}$ = 2.5, KIE$_{-3,int}$ = 2, and KIE$_{-4,int}$ = 1.5. (b) Resulting tKIE(t) time courses for each of the components are shown. The intercept of each curve on the $t = 0$ axis defines tKIE^0 for that reaction component.

where $tKIE_i^0$ is defined as

$$\lim_{t \to 0} tKIE_n(t)$$

for the nth step.

Thus, $tKIE_n^0$, the transient-state KIE evaluated at $t = 0$, is the arithmetic product of the numerical values of the KIE_{int}s of every forward step leading to the component that results from the nth step. Such a $tKIE^0$ value is not affected by KIE_{int}s of any step in the sequence later than n, nor do KIE_{int} effects on any reverse rate constant in the sequence contribute to its value. It can be seen that this theorem is consistent with and encompasses the special case of single-step substitution.

While eq 15 predicts the experimentally observed $tKIE_i^0$ for any given intermediate in a sequential reaction, eq 16 leads to a second theorem that provides a means of evaluating the intrinsic KIE for the forward rate constant of each individual step in the reaction sequence. On the basis of the result of eq 15 that the $tKIE^0$ for any given intermediate is the arithmetic product of the $tKIE^0$ values of all of the preceding steps, it follows that

$$KIE_{i,int} = \frac{\prod_{i=1}^{n} KIE_i^0}{\prod_{i=1}^{n-1} KIE_i^0} \qquad (16)$$

Combining eqs 15 and 16 gives

$$KIE_{n,int} = tKIE_n^0 / tKIE_{n-1}^0 \qquad (17)$$

Simply stated, the intrinsic KIE for any given step in a reaction is the $tKIE^0$ for that step divided by the $tKIE^0$ of the immediately preceding step.

The third theorem states that $tKIE_X^0$ is independent of KIE_{int} effects from any step in the reverse direction. Affirmation of these three theorems is provided by comparing the $t = 0$ intercepts of the curves shown in Figure 11b with the given values of the $KIE_{X,int}$ for the corresponding forward rate constant of the step leading to species X. Proof of the three theorems is provided by comparing the $t = 0$ intercept ($tKIE_X^0$) of each component with the given value of its $KIE_{X,int}$ value in the figure caption. A somewhat more satisfying proof is provided by the integration of the differential equations of the A ⇌ B ⇌ C reaction (the most complex reversible reaction scheme for which a closed integral can be obtained). As we have recently shown,[27] the values of

$$\lim_{t \to 0} \frac{d[B_H]/dt}{d[B_D]/dt}$$

and

$$\lim_{t \to 0} \frac{d[C_H]/dt}{d[C_D]/dt}$$

in this case can be obtained algebraically. The results are in perfect accordance with all three of our theorems.

Conclusions

The dependence of transient-state phenomena on both the time and signal source, in contrast to steady-state parameters, which are independent of both, has two important consequences. The loss of the applicability of the extensive body of rigorous algebraic theory of the steady state is more than compensated by an enormous increase in the scope of directly observable physical phenomena. This scope is limited only by the inherent properties of a specific enzyme reaction and the ingenuity of the experimentalist. The opportunity to exploit this underused approach to attain a completely new level of mechanistic understanding has been severely limited by the lack of a rigorous and applicable body of theory. In this Account, we have tried to propose a few basic elements of such a theory. Its full development awaits the future.

References

(1) Westheimer, F. H. 1949 (personal communication).
(2) Cleland, W. W. *The Enzymes,* 3rd ed.; Academic Press: New York, 1991; pp 99–158.
(3) Hermes, J. D.; Roeske, C. A.; O'Leary, M. H.; Cleland, W. W. Use of Multiple Isotope Effects To Determine Enzyme Mechanisms and Intrinsic Isotope Effects. Malic Enzyme and Glucose-6-phosphate Dehydrogenase. *Biochemistry* **1982**, *21*, 5106–5114.
(4) Hiromi, K. *Kinetics of Fast Enzyme Reactions*; Halsted Press: Tokyo, Japan, 1979.
(5) Johnson, K. *Kinetic Analysis of Macromolecules: A Practical Approach*; Oxford University Press: Oxford, U.K., 2003.
(6) Moore, J. W.; Pearson, R. G. Kinetics and Mechanism. John Wiley and Sons: New York, 1981; pp 296–300.
(7) Schopfer, L. M.; Massey, V.; Ghisla, S.; Thorpe, C. Oxidation–Reduction of General Acyl-CoA Dehydrogenase by the Butyryl-CoA/Crotonyl-CoA Couple. A New Investigation of the Rapid Reaction Kinetics. *Biochemistry* **1988**, *27*, 6599–6611.
(8) Bernasconi, C. F. *Relaxation Kinetics*; Academic Press: New York, 1976.
(9) Maniscalco, S. J.; Saha, S. K.; Fisher, H. F. Identification and Characterization of Kinetically Competent Carbinolamine and α-Iminoglutarate Complexes in the Glutamate Dehydrogenase-Catalyzed Oxidation of L-Glutamate Using a Multiwavelength Transient State Approach. *Biochemistry* **1998**, *37*, 14585–14590.
(10) Fisher, H. F. *Transient State Kinetic Approaches to the Resolution of Enzyme Mechanisms*; IOS Press: Amsterdam, The Netherlands, 1998; pp 264–277.
(11) Tally, J. F.; Maniscalco, S. J.; Saha, S. K.; Fisher, H. F. Detection of Multiple Active Site Domain Motions in Transient-State Component Time Courses of the *Clostridium symbiosum* L-Glutamate Dehydrogenase-Catalyzed Oxidative Deamination Reaction. *Biochemistry* **2002**, *41*, 11284–11293.
(12) Saha, S. K.; Maniscalco, S. J.; Singh, N.; Fisher, H. F. The Demonstration of a Glutamate Dehydrogenase–NADP–L-Glutamate Charge-Transfer Complex and Its Location on the Reaction Pathway. *J. Biol. Chem.* **1994**, *269*, 29592–29597.
(13) Fisher, H. F.; Maniscalco, S.; Singh, N.; Mehrotra, R. N.; Srinivasan, R. A Slow Obligatory Proton Release Step Precedes Hydride Transfer in the Liver Glutamate Dehydrogenase Catalytic Mechanism. *Biochim. Biophys. Acta* **1992**, *1119*, 52–56.
(14) Singh, N.; Maniscalco, S. J.; Fisher, H. F. The Real-Time Resolution of Proton-Related Transient-State Steps in an Enzymatic Reaction. The Early Steps of the Oxidative Deamination Reaction of Bovine Liver Glutamate Dehydrogenase. *J. Biol. Chem.* **1993**, *268*, 21–28.
(15) Srinivasan, R.; Viswanathan, T. S.; Fisher, H. F. Mechanism of Formation of Bound α-Iminoglutarate From α-Ketoglutarate in the Glutamate Dehydrogenase Reaction. A Chemical Basis for Ammonia Recognition. *J. Biol. Chem.* **1988**, *263*, 2304–2308.

(16) Fisher, H. F.; Srinivasan, R.; Rougvie, A. E. Glutamate Dehydrogenase Catalyzes the Reduction of a Schiff Base (δ-1-Pyrroline-2-carboxylic Acid) by NADPH. *J. Biol. Chem.* **1982**, *257*, 13208–13210.

(17) Srinivasan, R.; Fisher, H. F. Deuterium Isotope Effects for the Non-enzymatic and Glutamate Dehydrogenase Catalyzed Reduction of an α-Imino Acid by NADH. *J. Am. Chem. Soc.* **1985**, *107*, 4301.

(18) Rife, J. E.; Cleland, W. W. Determination of the Chemical Mechanism of Glutamate Dehydrogenase From pH Studies. *Biochemistry* **1980**, *19*, 2328–2333.

(19) Stillman, T. J.; Baker, P. J.; Britton, K. L.; Rice, D. W. Conformational Flexibility in Glutamate Dehydrogenase. Role of Water in Substrate Recognition and Catalysis. *J. Mol. Biol.* **1993**, *234*, 1131–1139.

(20) Fisher, H. F. A Unifying Model of the Thermodynamics of Formation of Dehydrogenase–Ligand Complexes. *Adv. Enzymol. Relat. Areas Mol. Biol.* **1988**, *61*, 1–46.

(21) Eftink, M. R.; Biltonen, R. L. In *Biological Microcalorimetry*; Breezer, A. E., Ed.; Academic Press: New York, 1980.

(22) Saha, S. K.; Fisher, H. F. The Location of Active Site Opening and Closing Events in the Prehydride Transfer Phase of the Oxidative Deamination Reaction Catalyzed by Bovine Liver Glutamate Dehydrogenase Using a Novel pH Jump Approach. *Biochim. Biophys. Acta* **1999**, *1431*, 261–265.

(23) Maniscalco, S. J.; Saha, S. K.; Vicedomine, P.; Fisher, H. F. A Difference in the Sequence of Steps in the Reactions Catalyzed by Two Closely Homologous Forms of Glutamate Dehydrogenase. *Biochemistry* **1996**, *35*, 89–94.

(24) Vanhooke, J. L.; Thoden, J. B.; Brunhuber, N. M.; Blanchard, J. S.; Holden, H. M. Phenylalanine Dehydrogenase from *Rhodococcus* sp. M4: High-Resolution X-ray Analyses of Inhibitory Ternary Complexes Reveal Key Features in the Oxidative Deamination Mechanism. *Biochemistry* **1999**, *38*, 2326–2339.

(25) Fisher, H. F.; Bard, J. R.; Prough, R. A. Transient-State Intermediates Involved in the Hydride Transfer Step of the Glutamate Dehydrogenase Reaction. *Biochem. Biophys. Res. Commun.* **1970**, *41*, 601–607.

(26) Fisher, H. F.; Saha, S. K. Interpretation of Transient-State Kinetic Isotope Effects. *Biochemistry* **1996**, *35*, 83–88.

(27) Maniscalco, S. J.; Tally, J. F.; Fisher, H. F. The Interpretation of Multiple-Step Transient-State Kinetic Isotope Effects. *Arch. Biochem. Biophys.* **2004**, *425*, 165–172.

(28) Fisher, H. F.; Maniscalco, S. J. A Close-Packed Planar 4-Atom Motif Serves as a Variable-Pathway Mechanistic Switching Device in Enzymatic Catalysis. *Bioorg. Chem.* **2002**, *30*, 199–210.

AR040218G